COLLOIDAL ORIGIN OF COLLOFORM-BANDED TEXTURES IN THE LOW-SULFIDATION, SEDIMENTARY ROCK-HOSTED AU-AG KHAN KRUM (ADA TEPE) DEPOSIT, SE BULGARIA

Irina Marinova[1], Rositsa Titorenkova[1], Valentin Ganev[1]

[1]*Institute of Mineralogy and Crystallography, Bulgarian Academy of Sciences, Acad. G. Bonchev Str., Bl. 107, 1113 Sofia, Bulgaria, irimari@gmail.com*

Abstract

The paper presents data on both colloform-banded macro- and micro-texture from the Au-Ag Khan Krum deposit. The macro-texture characterises with obscured boundaries of bands, a finer inner banding, a strongly prevailing random-grain fabrics of quartz and adularia, re-crystallization of quartz and adularia, pores of syneresis lined with comb quartz and adularia, and presence of feathery and fibrous quartz that is why we presume formation from colloidal solutions resulted most probably from intense boiling of fluids. For the micro-banding of bonanza electrum we suppose deposition from more concentrated colloidal solutions than that in the macro-bands, most likely due to extreme boiling of fluids in open or quasi open hydrothermal system. The dendrite- and chain-like electrum aggregates, as well as the oval clots are related to reorientation of aggregated electrum globules during plastic deformation of a mixed ore-silicate gel for the high angles of the veins. Electrum has not been deposited into pores and cracks of syneresis, what indicates that it had been a sol. For the dense sprinkles of electrum globules on the surfaces of some bands, we infer condensation of gaseous phase separated during the boiling of fluids.

Key words: colloform-banded textures, cracks and pores of syneresis, electrum, adularia, vein quartz

INTRODUCTION AND PROBLEM

The detailed studies of colloform textures by Grigor'ev [1], Lebedev [2], Roedder [3], etc., have revealed that these textures could form either via crystallization from true solutions or via crystallization and re-crystallization from gels. Additionally, it is well known that the crystallization and diagenesis of gels erase their colloidal stage. Thus, when the colloform textures have been formed by a primary deposition of opal or chalcedony it is very difficult to decipher their origin due to the crystallization of opal and chalcedony into the more stable quartz (Herdianita et al. [4]). In these cases only some textural and morphological features of the metacolloidal minerals testify to their colloidal origin.

First illustrations of colloform-banded textures from the Khan Krum deposit have been presented by Marchev et al. [5] and Jelev [6], who outlined their bonanza gold grades and displayed visible gold. Marchev et al. [5] have accepted colloidal origin of these textures based on the presence of opal and dendritic gold. Later, Marinova [7] has pointed that high-grade electrum in the colloform-banded textures is deposited in their finest quartz-adularia bands, forms aggregates without own crystal faces, and can be related to intense boiling of hydrothermal fluids.

The objective of this paper is to describe the mineral composition, textural and morphological features of colloform-banded textures from the Khan Krum deposit, as well as to advance reliable arguments in favour of their colloidal origin.

MATERIAL AND METHODS

The studied hand specimens of colloform-banded textures were collected in 2007 and 2008, and came from 10 bonanza high-angle veins cropping out mainly on the summit of the Ada Tepe ridge. The textural and morphological investigations were fulfilled with a stereomicroscope, a conventional polarizing optical microscope, and a scanning electron microscope (SEM) in secondary electrons at a voltage of 25 kV. For identifying the silica phases, powder samples were investigated using the powder X-ray diffraction method by a Dron-3M diffractometer operating at λ=0.17903 nm (cobalt radiation), 35 kV, 25 mA and with an iron filter for the range from 8 to 70° 2θ. For identifying the micro-sized apparently isotropic silica vibration spectroscopy was applied on polished thin sections. Micro-

Raman spectra were recorded by a LabRam Jobin-Ivon spectrometer equipped with an Olympus BX41 microscope and a He-Ne laser at wavelength of 633 nm. The beam power on the sample surface was 0.7 W, while the spectral resolution was 2 μm. For identifying of water in bonanza micro-bans we used Fourier transform infrared spectroscopy (FTIR) by FTIR Tensor-37 spectrometer coupled with Hyperion 2000 infrared microscope. Specular reflectance spectra in the range 4000-500 cm^{-1} from 100x100 μm selected areas of the sample surface were measured using a Schwarzschild objective (x15).

GEOLOGY

The Khan Krum deposit is located in the Eastern Rhodope Mountain, SE Bulgaria. The deposit has been discovered and explored by Balkan Mineral and Mining. The Khan Krum deposit comprises most of the precious-metals reserves of the Krumovgrad goldfield: 25 t gold at 5.07 g/t grade and 13 t silver at 2.7 g/t grade, amounts intended to be taken-by using open-pit mining (Jelev [6]). The regional and local geology are described in detail by Marchev et al. [5], Jelev [6], Marinova [7], Marton et al. [8]. That is why here are cited only the main characteristics of the deposit and some newly published data. The Khan Krum deposit is situated on the summit of the Ada Tepe ridge, in the upper plate of the regional low-angle Tokachka detachment fault (Bonev [9]). The host rocks are Maastrichtian-Paleocene breccia-conglomerates, breccias and sandstones filling the East-Rhodopian Paleogene Depression (Goranov et al. [10]), which lies on the northern periphery of the extensional Kessebir gneiss dome (Bonev [11]). The Au-Ag mineralization is covered by non-mineralized Upper-Eocene sediments (Jelev, Hasson [12]). The Kessebir dome comprises metamorphic rocks of two structural complexes – lower and upper (Bonev [11]). The age of protoliths of the upper complex (amphibolites, gneisses, schists, marbles, ultramafites), determined by U-Pb LA-ICP/MS zircon geochronology, is Ordovician (Bonev et al. [13]). The Rb-Sr ages of 328±25 Ma (Carboniferous) were obtained for the lower complex, dominated by igneous protoliths (Peycheva et al. [14]). The isotopic ratio 40Ar/39Ar for metamorphic rocks from the lower complex indicates a cooling process via exhumation through detachment faulting down to 350° C, happened in a period between 37.28±0.19 Ma and 36.90±0.16 Ma. The sedimentary rock-hosted gold-silver mineralization had developed from 35.36±0.0.21 Ma to 34.71±0.0.16 Ma. Thus, the earliest known calc-alkaline type magmatism at the near-by Iran Tepe volcano (33.97±0.36 Ma to 34.62±0.46 Ma) almost coincides with the end of the hydrothermal mineralization (Marton et al. [8]). A study of Bonev et al. [15] has presented similar values for the 40Ar/39Ar ages.

The mineralization of the Khan Krum deposit is epithermal, low-sulfidation, with electrum being the only economic mineral (Kunov et al. [16]; Marchev et al. [5]; Jelev [6]); Marinova [7]). The fluids have been of temperature 250-220° C; of low salinity (Marton et al. [17]), and dominated by meteoric water, partly re-equilibrated with metamorphic and magmatic basement rocks (Moritz et al. [18]). The hydrothermal alteration of the host rocks is of fault-controlled adularia-sericite type (Kunov et al. [16]).

The styles of mineralization include: 1) low-angle layer-like bodies of replacement; 2) stockwork bodies, and 3) high-angle open-space filling veins.

RESULTS AND DISCUSSION

Colloform-banded macro-texture

Field, macroscopic, and stereomicroscopic observations

The studied colloform-banded veins reach maximum width of 50 cm, but usually they are only a few centimetres wide, and are presented by alternating bands coloured milky, water-clear, pale-grey, and pale-beige. The width of the individual bands varies commonly from a few millimetres up to several centimetres (Fig. 1, 2). When observed by naked eye, the bands display clear, sharp boundaries, which are healed and sealed, and porcelain-like appearance. The colloform-banded veins are highly cracked as the filled cracks are healed and sealed reflecting the significant role of hydraulic fracturing (Phillips [19]) in the development of the colloform-banded veins; the multiple cross-cutting relations of veinlets being an evidence for multiple episodes of hydraulic fracturing and mineral deposition. Stockwork cracks of some bands do not pass

into the next bands, thus displaying the formation of individual bands one after another (Fig. 2).

A characteristic feature of the colloform-banded texture is the rounded, botryoidal surfaces of the individual bands. The bands differ significantly in texture from one another: there are both massive bands and such with a finer inner banding due to the alternation of differently coloured bands. In some places, this finer banding shows periodic features (Fig. 2). In the studied colloform-banded textures, everywhere there are voids that look like oval primary millimetre-scaled pores, centimetre-scaled empties, and cracks of exfoliation up to 1 mm wide.

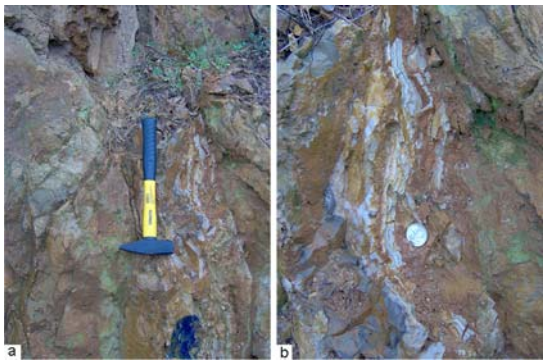

Figure 1. High-angle vein on the summit of the Ada Tepe ridge: **a** colloform-banded vein; **b** detail from a – clearly seen colloform shapes of individual bands.

Some bands are entirely composed of the lattice-bladed texture (Fig. 2d) (presumable replacement of quartz and adularia after platy calcite; Simmons, Christenson [20]; Dong et al. [21]). The substantial differences in the texture of bands are an additional evidence for their formation from individual hydrothermal pulses one after another.

Observations under optical microscope

In transmitted light, the boundaries of the individual colloform macro-bands are seen of various degree of contrast. At small magnifications, with contrast boundaries are visualized the bands differing significantly in the intensity of brown pigmentation, in the abundance of scattered dusty opaque micro-inclusions, in the quartz-to-adularia ratio, and in their grain size. At higher magnifications, the band boundaries are unclear and uneven (Fig. 3a). Further, in the bands, there is a random growth of the constituent minerals on the host rocks or on the preceding band. The main minerals (quartz and adularia) of the band matrix are arranged in spots, indicating re-crystalization (Fig. 3b). Additionally, one observes a lot of micro-pores, lined with quartz and adularia microdruses considerably coarser then the matrix, where both quartz and adularia crystals show geometrical selection, that is a feature characteristic of crystallization from true solutions (Fig. 3c).

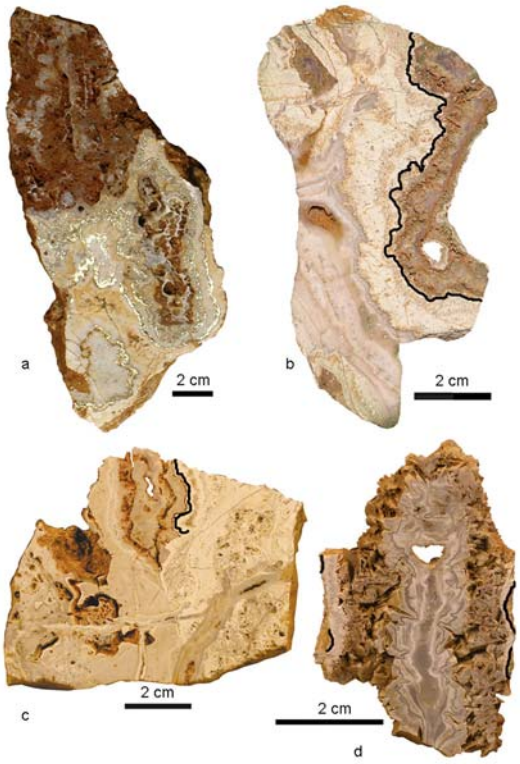

Figure 2. Hand specimens of colloform-banded macro-texture. The black lines in b, c, and d are not properly scaled and are superimposed over submillimetre-wide bands of bonanza electrum grades: **a** quartz-adularia vein containing visible electrum (white bands) (by courtesy of D. Jelev). There seen are a lot of oval voids. Filled hair-line joints are seen in the lowest quarter of the specimen. Supergene goethite (black); **b** colloform-banded vein containing a submillimetre-wide electrum-rich band. The colour of the middle band is due to abundance of adularia. In the left band, there is an alternation of milky-coloured, pale-grey and water-clear bands forming finer inner banding. In both bands one sees stockwork hair-line quartz veinlets, missing in the right end; **c** colloform-banded vein with a submillimetre-wide bonanza electrum band and a few cracks of exfoliation. The right half of the specimen contains abundant adularia. A quartz veinlet down in the right; **d** in the central part, there is a colloform band of finer inner banding whose milky-coloured bands contain dispersed electrum clots, outwards symmetrically bands of a lattice-bladed texture are seen, followed by quartz-adularia bands, both ending with a sub-millimetre-wide colloform band of bonanza electrum grades (black).

The colloform macro-bands are composed of microcrystalline, nearly equigranular quartz and adularia, whose ratio and grain-size vary from band to band. One recognizes almost adularia, almost quartz, and mixed quartz-adularia bands. The macro-bands contain as well as disseminated electrum and pyrite, feathery and fibrous quartz, and dusty opaque micro-inclusions.

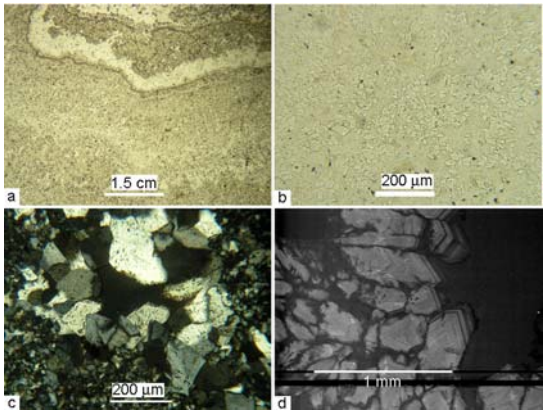

Figure 3. Photomicrographs of colloform-banded macro-textures (a-c in transmitted light, d in SEM-CL): **a** boundaries of bands displaying different contrast. //N; **b** spotty distribution of quartz and adularia (pseudorhombic). //N; **c** a pore lined with quartz and adularia (rhombic outlines) crystals, displaying geometrical selection. +N; **d** SEM-CL of euhedral quartz crystals (lining a micro-pore) displaying clear oscillatory zonality of growth.

Adularia is pale-beige and its abundance varies over a wide range, from 3 to 50 vol. % (commonly being 30-50 vol. %). Approximately equigranular adularia grains of anhedral and isometric outlines, sized below 20-30 µm, sharply prevails in the macro-bands, inter-grown with coarser, predominantly geometrically selected adularia grains of subhedral and euhedral shape of rhombic outlines, and with a size up to 200-300 µm, that occur in thin bands and spots or deposited in micro-pores (Fig. 3c). Pseudorhombic adularia is an indicator of boiling of fluids (Browne [22]; Dong, Morrison [23]).

Quartz in the colloform macro-bands is presented by milky, pale-grey, and water-clear varieties and a quantity from 50 up to 97 vol. %. Commonly, likely adularia, it is sized up to 20-30 µm, and is anhedral and isometric, with its coarser grains reaching about 200 µm, and being of subhedral or euhedral habit. Generally, in all coarser quartz grains, one observes arrangement in spots, finer bands, and lining micro-pores (Fig. 3c). In the latter case, the quartz crystals often display feathery texture, zonality, a growth at high angle to the substrate, and a geometrical selection. The feathery texture is due to abundance of fluid inclusions sized below 1 µm that occur as oriented trails, and is typical for the epithermal quartz (Dong et al. [22]). The zoned quartz from micro-pores displays in the cathode-luminescence (CL) images a clear oscillatory zonality of crystallographic orientation, drawn by alternating dark-grey and light-grey luminescent bands (Fig. 3d). Occasionally, contacting quartz crystals display areas of pervasive fibrous texture, thus revealing their formation via re-crystallization of a fibrous precursor. Feathery and fibrous textures of quartz are commonly accepted as indicative of re-crystallization, chalcedony being the most suspected primary mineral (Lebedev [2]; Sander and Black [24]; Dong et al. [21], etc.).

As shown above, the major volume of colloform macro-bands is of quartz-adularia composition and of random-grain fabrics both within the bands and on their boundaries. Thus, the missing comb texture there, combined with random-grain fabrics, a finer periodic banding in some macro-bands, and obscured boundaries indicate that the macro-bands can hardly be formed from true solutions rather speaks in favour of crystallization from a silicate gel. The differentiation of quartz and adularia from one another into almost mono-mineral spots could be explained with re-crystallization characteristic of crystallization from gels (Lebedev [2]).

The overall distribution of millimetre- to sub-millimetre-sized pores, lined with relatively coarse comb, euhedral and subhedral quartz and adularia, and the lack of feeding channels (cracks) for fluids, all means that the former are pores of syneresis. Thus, it is reasonable to conclude that true solutions, being separated during the drying of, and the crystallization from a silicate gel, have passed through the gel like through a semi-permeable membrane (Quincke [25]), entered the pores, and then deposited coarser quartz and adularia under conditions of geometrical selection.

In the studied colloform-banded macro-textures electrum (sized below 20-30 µm) and pyrite (up to 50 µm in size and up to 3 vol. %) form dispersed grains, interstitial to and intergrown with quartz and adularia, together with scarce flakes of sericite (below 1 vol. %).

Colloform micro-banding

Observations under optical microscope

The micro-banding is of millimetre- to sub-millimetre range, appearing as a series of micro-bands with a total width of 1-2 mm, but mostly being of a sub-millimetre width. Commonly, these series are concordant to the neighbouring macro-bands (Fig. 2), but there are such of discordant position. The series appear an alternation of about 10-30 individual quartz-adularia micro-bands, varying in width from 10 to about 500 μm. Commonly, quartz and adularia grains are sized below 3-5 μm and are of isometric, anhedral outlines. In many hand specimens, some micro-bands are composed of adularia and apparently isotropic silica (Fig. 4a). As a rule these micro-bands are rich in electrum of quantity up to 50 vol. %, which aggregates occasionally are visible by naked eye. The micro-bands rich in electrum contain also dense dusty opaque micro-inclusions, which seem to be also of electrum. Adularia in the electrum-rich micro-bands is also of high abundance (50-80 vol. %). Besides mixed silica-adularia micro-bands, almost mono-mineralic quartz micro-bands occur as well. Somewhere in the micro-banding, sub-millimetre spheres occur (Fig. 4b), corresponding to quartz according to the powder X-ray diffraction data, together with unfilled cracks parallel to the bands. The micro-banding forms contrast margins with the neighbouring macro-bands, thus indicating formation from an individual hydrothermal pulse. At the same time, its margins are uneven and without clear marks of partition (Fig. 4a-b).

Like the macro-bands discussed so far, the individual micro-bands differ in their grain size, porosity, quartz-to-adularia ratio, the quantity of scattered dusty opaque micro-inclusions, abundances of electum and pyrite, and the presence/absence of brown pigmentation. Besides the prevailing contrasted boundaries of the micro-bands, an unclear micro-banding is also observed, named by Saunders [26] “pseudo-sedimentary texture”, with textures presented in our thin sections by diffusive and gradational margins (Fig. 4c). These features are indicative of a primary gel consistency of the matter forming the major part of the colloform-banded micro-textures.

Two types of orientation of the quartz and adularia crystals occur in the micro-bands: 1) randomly oriented grains that characterize the major part of the micro-banding, and 2) grains oriented approximately perpendicularly to preceding band, thus forming a comb texture that plays a subordinated role. We suppose that the random-grain fabrics of quartz and adularia (just like in the macro-bands) reflects a colloidal origin. In the second type of orientation, a geometrical selection has acted, revealing that the crystals have been deposited via direct crystallization.

Sporadically, in the millimetre-to-submillimetre-wide banding, there arise spherolites which usually display a radial texture in their outer parts, while their central parts are built up of anhedral quartz (Fig. 4d). Quartz of some spherolites is co-grown with fine pseudorhombic adularia crystals. We interpret these shapes as coming from former chalcedonic spherolites.

Similarly to the colloform-banded macro-textures, in individual micro-bands, fibrous quartz occurs in quartz-adularia matrix in quantity, which commonly does not exceed 3 vol. %, occasionally reaching to 10 vol. %. Most probably, the fibrous quartz is a transformation of chalcedony into quartz with preservation of the former fibrous texture in places.

Electrum in the bonanza micro-bands forms: 1) micron-sized dendrite-like aggregates or closely disposed oval aggregates that form tree- and chain-like shapes, orientated most often transversely or obliquely to the banding; 2) relatively coarse clots along the banding and in places reaching sizes visible by naked eye; 3) disseminated micron-sized grains, and 4) dense sprinkles of micron-sized electrum globules deposited in open space on surfaces of micro-bands.

The transverse electrum aggregates are predominantly located in protruded parts of colloform micro-bands and everywhere intersecting only a few neighbouring micro-bands, never the entire banding, being covered by the next bands, without any feeding cracks. These observations mean that the source of electrum is not external for the micro-banding, but is internal. In reflected light, it is plainly visible that the colloform micro-banding is breached by material containing electrum dendrites, being developed transversely (Fig. 4e). The absence of clear margins between the

transverse in-filling and host micro-bands means that during breaching the matrix was not solidified but being still viscous.
The electrum clots, tracing the micro-banding, occur as oval aggregates concentrated in a few neighbouring quartz-adularia micro-bands, the largest of them lie on the bands bottom. Somewhere, euhedral quartz crystals are covered by bended globular electrum aggregate, a fact suggesting that during the quartz crystallization the electrum aggregate was still viscous (Fig. 4f - insert).
In places, electrum is inter-grown with pyrite in the sense that it overgrows pyrite but occurs also in the pyrite therein as small grains. These observations reveal a crystallization of electrum and pyrite from an ore-silicate gel.

Vibration spectroscopy

We studied micro-banding containing apparently isotropic silica by micro-Raman spectroscopy and obtained the typical Raman spectrum of α-quartz, which contains in the spectral range 100-600 cm^{-1} seven pronounced peaks at about 126, 204, 262, 353, 400, 463, and 511 cm^{-1} (Kingma and Hemley [27]). The FTIR-investigations have shown that the H_2O and OH characteristic bands typical for opals were not observed in the MIR region. The results obtained from the vibration spectroscopy revealed that the silica in the micro-banding is presented only by quartz.

Observations in secondary electrons

In secondary electrons, the images of millimetre-to-submillimetre-wide colloform-banded texture, cut perpendicularly to the banding, exhibit an alternation of poorly crystalline micro-bands and such of clear crystallinity. The first ones appear with a varying crystallinity, looking in secondary electrons like vitreous, and black or dark grey in colour, shortly denoted vitreous-like. The second ones look light grey, denoted crystalline (Fig. 5a-b). Besides crystalline micro-bands there exist also crystalline micro-pores. The crystalline micro-bands and micro-pores are lined with quartz and adularia crystals, which display geometrical selection and well-developed faces.
The electrum aggregates, cut near their base, exhibit a lace-like texture due to the abundance of angular pores occupied by quartz and adularia.

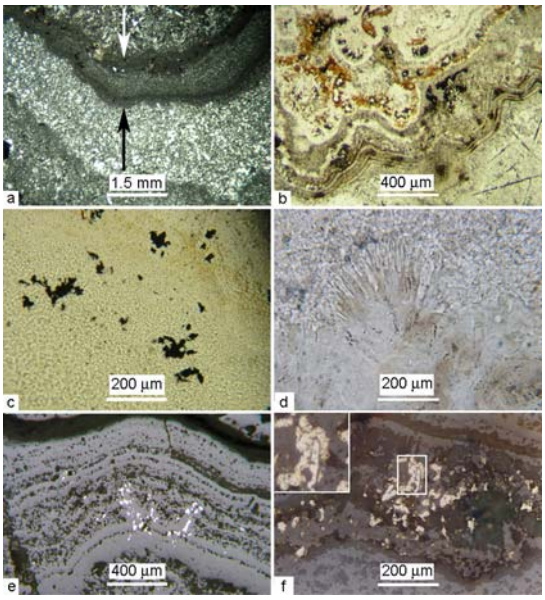

Figure 4. Photomicrographs of colloform-banded micro-textures (a-d in transmitted light, e-f in reflected light): **a** series of micro-bands (between the arrows); the outer micro-bands (black) consisting of apparently isotropic silica. +N; **b** quartz-adularia micro-bands very rich in electrum spots and micro-layers along the banding (black). A spherical texture composed of quartz and electrum (black) in the upper left part, and linear voids of dissolved platy calcite in-filled with black opaque material in the lower right corner. //N; **c** grain-size gradation, random-grain fabrics of quartz and adularia, and transverse electrum dendrite-like aggregates (black). //N; **d** quartz spherolite covered by quartz-adularia micro-bands. //N; **e** transverse fan-like electrum aggregates (white) developed only in several micro-bands in their protruded portion. +N; **f** electrum clots in micro-banding. Insert – euhedral quartz crystal covered by bended globular electrum aggregate. +N.

The optical observations and the SEM-images of colloform-banded micro-textures allow us to conclude that: (i) the crystalline micro-pores and micro-bands are, respectively, pores and cracks of syneresis, (ii) the quartz and adularia micro-crystals, deposited on their walls, have been deposited from true solutions which have passed through the silicate gel like through a semi-permeable membrane, and (iii) the overall absence of electrum within the crystalline micro-pores and micro-bands reveals that electrum has not been deposited from true solutions rather from colloids.
As afore-mentioned, in some instances, there are sprinkles of globular electrum observed on the surface of some micro-bands, which are obviously grown in open space. Most likely, the electrum sprinkles appear condensates of gasses separated during the boiling of fluids.

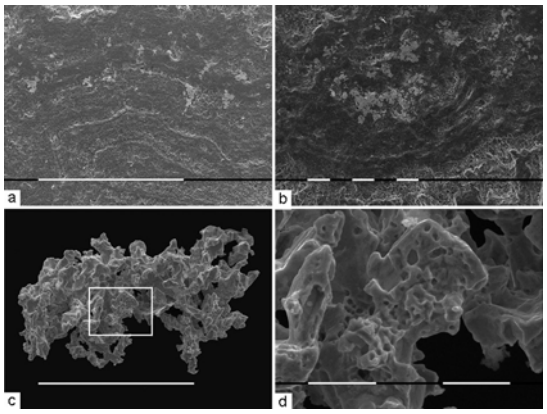

Figure 5. Electrum in secondary electrons: **a** alternation of clearly crystalline (grey) and vitreous-like (black) micro-bands with transverse electrum aggregates (light grey); **b** alternation of vitreous-like micro-bands (black) and crystalline ones (light grey), and electrum clots occurring only in vitreous-like micro-bands on the bottom of a concave portion of the banding; **c** electrum aggregate abundant in oval micro-concavities; **d** detail from (c). Scale bar: a 1 mm, b-c 100 μm, d 10 μm.

Electrum liberated from the silicate matrix with hydrofluoric acid, shows platy shapes with very uneven surface. At high magnifications, the surface of plates looks like dough with a lot of oval voids visible on their surface, which are negative prints of the globular shape of silicate gel (Fig. 5c-d).

CONCLUSSIONS

1. The main differences between the macro- and the micro-texture are in the abundances of adularia and electrum, and in their grain size; in the extent of re-crystallization and of the participation of cracks of syneresis.

2. We relate the greater extent of re-crystallization of the macro-texture than that of the micro-texture to the formation of the former from colloidal solutions of a larger water amount and the respective richer in water gel, than those responsible for the formation of the latter. The colloform-banded macro-texture we relate to intense boiling of fluids in closed or quasi closed hydrothermal system, while the bonanza colloform micro-banding – to open or quasi open system.

3. On the base of the textural analysis performed, we describe schematically the formation of the bonanza of electrum colloform-banded texture into a few generalized stages: (i) Filling of millimetre-to-submillimetre-wide joints with an ore-silicate sol; (ii) Coagulation of the sol and precipitation of a banded silicate gel. Electrum aggregation into micron-sized globules and coarser clots disseminated within the silicate gel; (iii) Drying and compaction of the banded gel and formation of pores and cracks of syneresis. Formation of colloform surfaces; plastic deformation of the gel under the action of gravity for the high angles of the joints. Simultaneous reorientation of aggregated electrum globules in transverse dendrite- and chain-like shapes into the protruded parts of the gel, and flowing down of coarse electrum clots into the concave parts, resulting from the huge difference between the specific weight of electrum and that of quartz and adularia; (iv) Crystallization of chalcedony, quartz and adularia and formation of their crystals into the still viscous electrum and its further reorientation forced from the crystallization of silicates. Lining of pores and cracks of syneresis with relatively coarse quartz and adularia crystals deposited from true solutions passing through the gel like through a semi-permeable membrane. Crystallization of electrum; (v) Diagenesis (re-crystallization and erasing of the gel textures).

ACKNOWLEDGEMENTS

The authors thank the colleagues from Balkan Mineral and Mining for their assistance during the work on the deposit. This study was financially supported in part by the National Science Fund of Bulgaria (DO-02-82/2008 project). This report is presented with the help of the project No BG051PO001-3.3-05/0001 (Science and Busyness), financed by the "Development of public relations" Operative Program.

REFERENCES

[1] Grigor'ev D., 1965: Ontogeny of minerals. Israel Program for Scientific Translations Ltd, Jerusalem.

[2] Lebedev L., 1967: Metacolloids in endogenic deposits. Plenum Press, New York.

[3] Roedder E., 1968: The Noncolloidal Origin of "Colloform" Textures in Sphalerite Ores. Econ. Geol., 63, 451-471.

[4] Herdianita N., Browne P., Rodgers K., Campbell K., 2000: Mineralogical and textural changes accompanying ageing of silica sinter. Miner. Deposita, 35, 48-62.

[5] Marchev P., Singer B., Jelev D., Hasson S., Moritz R., Bonev N., 2004: The Ada Tepe deposit: a sediment-hosted, detachment fault-controled, low-sulfidation gold deposit in the Eastern Rhodopes, SE Bulgaria. Schweiz. Mineral. und Petrogr. Mitt., 84, 59-78.

[6] Jelev D., 2007: Khan Krum gold deposit, Ada Tepe prospect. Gold deposits in Bulgaria. Zemya'93, Sofia, 104-115 (in Bulg.).
[7] Marinova I., 2008: Morphology of electrum from Khan Krum gold deposit, Krumovgrad goldfield, Eastern Rhodope Mountain, SE Bulgaria. Geol. Macedonica, 2, 111-120.
[8] Marton I., Moritz R., Spikings R., 2010: Application of low-temperature thermochronology to hydrothermal ore deposits: Formation, preservation and exhumation of epithermal gold systems from the Eastern Rhodopes, Bulgaria. Tectonophysics, 483, 240-254.
[9] Bonev N. 1996: Tokachka shear zone southwest of Krumovgrad in Eastern Rhodopes, Bulgaria: an extensional detachment. Ann. Univ. Sofia, 1–Geology, 89, 97-106.
[10] Goranov A., Kozhoukharov D., Boyanov I., Kozhoukharova E., 1995: Explanatory note to the geological map of Bulgaria at 1:100 000 scale, Krumovgrad and Sape map sheets. Avers, Sofia (in Bulg., abstract in Eng.).
[11] Bonev N., 2002: Structure and evolution of the Kessebir gneiss dome, Eastern Rhodope. Dissertaion, Univ. Sofia (in Bulg.).
[12] Jelev D., Hasson S., 2002: Geology of Khan Krum gold deposit. In: "Modern Problems of the Bulgarian Geology", Sofia, 58-59.
[13] Bonev N., Marchev P., Ovtcharova M., Moritz R., Ulianov A., 2010: U-Pb LA-ICP/MS zircon geochronology of metamorphic basement and Oligogene volcanic rocks from the SE Rhodopes: inferences for the geological history of the Rhodope crystalline basement. In: "Nat. Confer. Bulgarian Geol. Soc.", Sofia, 115-116.
[14] Peycheva I., Ovtcharova M., Sarov S., Kostitsin Y., 1998: Age and metamorphic evolution of metagranites from Kessebir reka region, Eastern Rhodopes – Rb-Sr isotope data. In: "XVI Congress CBGA", Vienna, p. 471.
[15] Bonev N., Spikings R., Moritz R., Marchev P., 2010: Timing of extensional exhumation of the Eastern Rhodope high-grade basement (Bulgaria): 40Ar/39Ar constraints. In: "Nat. Confer. Bulgarian Geol. Soc.", Sofia, 117-118.
[16] Kunov A., Stamatova V., Atanasova R., Petrova P., 2001: The Ada Tepe Au-Ag-polymetalic occurrence of low-sulfidation (adularia-sericite type) in the Krumovgrad district. Minno delo i geologia, 4, 16-20 (in Bulg.).
[17] Marton I., Moritz R., Marchev P., Vennemann T., Spangenberg J., 2006: Fluid evolution within Eastern Rhodopian sedimentary rock-hosted low-sulfidation epithermal gold deposits, Bulgaria. In: "Au-Ag-telluride-selenide deposits, the IGCP 486 2006 field workshop", Izmir, 116-123.
[18] Moritz R., Marton I., Chambefort I., Noverraz C., 2007: Diversity of epithermal gold ore formation in southeastern Europe: a record of a protracted 60 m.y.-long geodinamic and metallogenic evolution of the Tethyan arc. In: "Advances in Regional Geological and Metallogenic Studies in the Carpathians, Balkans, Rhodope Massif and Caucasus (Romania, Serbia, Bulgaria and Georgia)", SE Europe Geosci. Found., Bor.
[19] Phillips W., 1972: Hydraulic fracturing and mineralization. J. Geol. Soc. London, 128, 337-359.
[20] Simmons S., Christenson B., 1994: Origins of Calcite in a Boiling Geothermal System. Amer. J. Sci., 294, 361-400.
[21] Dong G., Morrison G., Jaireth S., 1995: Quartz Textures in Epithermal Veins, Queensland – Classification, Origin, and Implication. Econ. Geol., 90, 1841-1856.
[22] Browne P., 1978: Hydrothermal alteration in active geothermal fields. Ann. Rev. Earth and Planet. Sci., 6, 229-250.
[23] Dong G., Morrison G., 1995: Adularia in epithermal veins, Queensland: morphology, structural state and origin. Miner. Deposita, 30, 11-19.
[24] Sander M. and Black J., 1988: Crystallization and Re-crystallization of Growth-Zoned Vein Quartz Crystals from Epithermal Systems – Implications for Fluid Inclusion Studies. Econ. Geol., 83, 1052-1060.
[25] Quincke G., 1902: Die Oberflachen-spannung an der Grenze wasseriger Colloid-losungen von verschiedener Conzentration. Annalen der Physik, 314, 969-1045.
[26] Saunders J., 1990: Colloidal transport of gold and silica in epithermal precious-metal systems: Evidence from the Sleeper deposit, Nevada. Geology, 18, 757-760.
[27] Kingma K., Hemley R., 1994: Raman spectroscopic study of microcrystalline silica. Amer. Min., 79, 269-273.